EUKARYOTIC CELL, June 2007, p. 984–996 Vol. 6, No. 6
1535-9778/07/$08.00+0 doi:10.1128/EC.00061-07

Carbohydrate Metabolism in the *Toxoplasma gondii* Apicoplast: Localization of Three Glycolytic Isoenzymes, the Single Pyruvate Dehydrogenase Complex, and a Plastid Phosphate Translocator▽†

Tobias Fleige,[1] Karsten Fischer,[2] David J. P. Ferguson,[3] Uwe Gross,[1] and Wolfgang Bohne[1]*

Institute of Medical Microbiology, University of Göttingen, Kreuzbergring 57, Göttingen D-37075, Germany[1]; Institute for Biology, University of Tromsø, 9037 Tromsø, Norway[2]; and Nuffield Department of Pathology, University of Oxford, John Radcliffe Hospital, Headington, Oxford OX3 9DU, England[3]

Received 28 February 2007/Accepted 16 April 2007

Many apicomplexan parasites, such as *Toxoplasma gondii* and *Plasmodium* species, possess a nonphotosynthetic plastid, referred to as the apicoplast, which is essential for the parasites' viability and displays characteristics similar to those of nongreen plastids in plants. In this study, we localized several key enzymes of the carbohydrate metabolism of *T. gondii* to either the apicoplast or the cytosol by engineering parasites which express epitope-tagged fusion proteins. The cytosol contains a complete set of enzymes for glycolysis, which should enable the parasite to metabolize imported glucose into pyruvate. All the glycolytic enzymes, from phosphofructokinase up to pyruvate kinase, are present in the *T. gondii* genome, as duplicates and isoforms of triose phosphate isomerase, phosphoglycerate kinase, and pyruvate kinase were found to localize to the apicoplast. The mRNA expression levels of all genes with glycolytic products were compared between tachyzoites and bradyzoites; however, a strict bradyzoite-specific expression pattern was observed only for enolase I. The *T. gondii* genome encodes a single pyruvate dehydrogenase complex, which was located in the apicoplast and absent in the mitochondrion, as shown by targeting of epitope-tagged fusion proteins and by immunolocalization of the native pyruvate dehydrogenase complex. The exchange of metabolites between the cytosol and the apicoplast is likely to be mediated by a phosphate translocator which was localized to the apicoplast. Based on these localization studies, a model is proposed that explains the supply of the apicoplast with ATP and the reduction power, as well as the exchange of metabolites between the cytosol and the apicoplast.

Up to 20 to 30% of the world population is estimated to be chronically infected with the apicomplexan parasite *Toxoplasma gondii*. The parasite differentiates within the human host between tachyzoites and bradyzoites, which display distinct physiological features. Mature bradyzoites are adapted for lifelong persistence in their hosts and display an extreme reduction in growth rate, up to a complete arrest of the cell cycle (7). In contrast, tachyzoites, which are present during the acute phase of infection, are characterized by a fast duplication time of 6 to 8 h, indicating that this stage possesses effective pathways for nutrient acquisition and energy metabolism.

T. gondii possesses, like many other apicomplexan parasites, a nonphotosynthetic plastid, the so-called apicoplast. This organelle contains a 35-kb circular genome with similarities to plastid genomes from algae and is surrounded by four membranes. These features support the secondary endosymbiosis of a photosynthetic alga by the apicomplexan ancestor as the phylogenetic origin of the apicoplast (21, 32, 43, 51). Numerous nucleus-encoded proteins are imported into the apicoplast, aided by a bipartite presequence which is composed of a signal peptide and an adjacent transit peptide (23, 24, 39, 49).

The apicoplast is the location of several anabolic pathways, such as type II fatty acid synthesis and isoprenoid biosynthesis, whose cytosolic counterparts are absent in *Toxoplasma* and *Plasmodium* (2, 19, 40). Inhibition of the apicoplast's metabolic function or interference with its DNA replication is lethal for the parasite and, thus, is a potential target for the development of novel drugs (15, 40, 50, 52).

The biosynthetic pathways of the apicoplast require effective mechanisms to provide the organelle with carbon sources, ATP, and reduction power; however, the precise metabolic pathways have not been experimentally confirmed. In plant cells, the metabolisms of plastids and the cytosol are connected by a number of transport proteins which mediate the exchange of metabolites across the inner envelope membrane and which belong to the family of plastid phosphate translocators (pPTs). Two pPTs were recently identified in *Plasmodium* which are likely to mediate the exchange of C3, C5, and C6 intermediates between the cytosol and the plastid. One of the translocators was mapped to the outer membrane (*Plasmodium falciparum* outer membrane triose phosphate translocator [PfoTPT]), while the second (PfiTPT) most likely is located in the inner membrane, although a localization of the pPTs in the remaining two membranes (numbers 2 and 3) of the four-membrane layer could not be excluded (36). It was also demonstrated that

* Corresponding author. Mailing address: Institute of Medical Microbiology, University of Göttingen, Kreuzbergring 57, D-37075 Göttingen, Germany. Phone: 49-551-395869. Fax: 49-551-395861. E-mail: wbohne@gwdg.de.

† Supplemental material for this article may be found at http://ec.asm.org/.

▽ Published ahead of print on 20 April 2007.

TABLE 1. Glycolytic enzymes in *T. gondii*

Glykolytic enzyme	EC no.	ToxoDB gene ID no.	SignalP 3.0 prediction	GenBank accession no.	Confirmed localization(s)
Hexokinase	2.7.1.1	57.m00001	Nonsecretory		Cytosol
GPI	5.3.1.9	76.m00001	Nonsecretory		Cytosol
Phosphofructokinase I	2.7.1.11	49.m03242	Nonsecretory		
Phosphofructokinase II	2.7.1.11	42.m00123	Nonsecretory		Cytosol
Aldolase I	4.1.2.13	46.m00002	Nonsecretory		Cytosol
Aldolase II	4.1.2.13	46.m03956	Nonsecretory		
TPI I	5.3.1.1	42.m00050	Nonsecretory	DQ457194	Cytosol
TPI II	5.3.1.1	44.m02801	Signal peptide	DQ457193	Apicoplast
GAPDH I	1.2.1.12	80.m00003	Nonsecretory		Cytosol
GAPDH II	1.2.1.12	59.m00091			
PGK I	2.7.2.3	641.m00193	Nonsecretory	DQ451788	Cytosol
PGK II	2.7.2.3	41.m01331	Signal peptide	DQ457189	Apicoplast
PGM I	5.4.2.1	59.m03656	Nonsecretory		Cytosol
PGM II	5.4.2.1	113.m00016	Nonsecretory	DQ457187	
ENO2	4.2.1.11	59.m03410	Nonsecretory		Cytosol/nucleus
ENO1	4.2.1.11	59.m03411	Nonsecretory		Cytosol/nucleus
PK I	2.7.1.40	55.m00007	Nonsecretory		Cytosol
PK II	2.7.1.40	129.m00253	Signal anchor		Apicoplast

a central enzyme for the carbohydrate metabolism, the pyruvate dehydrogenase (PDH) complex, which converts pyruvate into acetyl coenzyme A (acetyl-CoA), localizes exclusively to the *Plasmodium* apicoplast (20). In contrast to plants, which possess both a mitochondrial and a plastid PDH complex, the *Plasmodium* genome, as well as the *Toxoplasma* genome, encodes only a single set of complete PDH genes.

We provide, in this study, experimental evidence that at least three glycolytic isoenzymes are targeted to the apicoplast, while the cytosol contains a complete set of glycolytic enzymes. The mRNA regulation of the complete set of glycolytic genes was compared between fast-replicating tachyzoites and in vitro-induced bradyzoites. Furthermore, we show, with the aid of antisera and by the expression of epitope-tagged full-length proteins, that the *Toxoplasma* PDH complex is absent from the mitochondrion and exclusively localizes to the apicoplast. Finally, we demonstrate that the plastid pPT of *T. gondii* (TgPT) localizes to the apicoplast and is encoded by a single gene. The putative roles of these proteins for the parasite's carbohydrate and energy metabolism are discussed.

MATERIALS AND METHODS

***T. gondii* strains and cultivation.** The parasites were cultivated in human foreskin fibroblasts as previously described (42). The transactivator-expressing *T. gondii* strain RH (TATi-1 parasites) was kindly provided by M. Meissner and D. Soldati (35) and used for transfection experiments. A clonal isolate of the RH strain was used for reverse transcriptase (RT)-PCR experiments.

In vitro stage conversion. Human foreskin fibroblasts were infected with *T. gondii* (strain RH) and cultivated in Dulbecco's modified Eagle's medium–1% fetal calf serum. After an incubation time of 4 h at 37°C in 5% CO_2, the medium was replaced with pH shift medium (pH 8.4) to induce bradyzoite differentiation (46) and the parasites were cultured at 37°C without CO_2. The medium was exchanged after 48 h in order to keep the culture at a constant pH. After 96 h of incubation, the cultures were used for RNA isolation. Successful induction of bradyzoite differentiation was confirmed by measuring the mRNA level of the bradyzoite marker bag1, which was found to be >500-fold increased in the in vitro bradyzoites compared to the tachyzoites. The mRNA level of the tachyzoite marker enolase II (ENO2) (8) was reduced to only 40% of the ENO2 expression level in tachyzoites. The lack of a more-pronounced repression of a tachyzoite-specific gene indicates that the in vitro bradyzoites have just started their development and still express significant levels of tachyzoite-specific genes.

RT-PCR. The total RNA was isolated by using a GenElute mammalian total RNA kit (Sigma) and treated with DNase I (Sigma) to remove any residual genomic DNA, according to the manufacturer's instructions. About 5 μg of the total RNA was reverse transcribed with Moloney murine leukemia virus RT (RNase H minus) from Sigma and with oligo$(dT)_{18}$, according to the manufacturer's protocol. Samples were used for light-cycler PCR using the primer pairs listed in Table S2 in the supplemental material. The primer pairs were designed using the DNAStar program. The annealing temperature was optimized by melting-curve analysis after the light-cycler PCR was performed, and the PCR products obtained were additionally analyzed by agarose gel electrophoresis for the presence of a single PCR product of the expected size. Furthermore, the primer pairs were tested on different cDNA amounts to confirm the linearity of the titration. The crossing-point values obtained for the tachyzoites and bradyzoites were normalized for actin mRNA expression.

Protein expression and purification. The *T. gondii* PDH subunits E1-beta and E2 were expressed in *Escherichia coli* strain BL21+ (Stratagene) by using the pQE-30 expression system (QIAGEN) with an N-terminal hexahistidine tag. The final expression constructs encoded amino acids 27 to 198 of E1-beta (20.6 kDa) and amino acids 444 to 669 of E2 (24.0 kDa). The expressed fragments were amplified from the cDNA of *T. gondii* strain RH using Phusion high-fidelity DNA polymerase (NEB) and primers with the BamHI/HindIII restriction sites listed in Table S1 in the supplemental material. The PCR fragments were subcloned in pCR4.0-Topo (Invitrogen), and the integrity of the open reading frames (ORFs) was confirmed by DNA sequencing. The fragments were finally cloned into pQE-30 (QIAGEN) by using the BamHI/HindIII restriction sites. Recombinant protein was obtained from the bacterial lysate and purified using Ni-nitriloacetic acid agarose (QIAGEN) under denaturating conditions (8 M urea), according to the manufacturer's protocol. The eluted fractions were analyzed by sodium dodecyl sulfate-polyacrylamide gel electrophoresis and immunoblotting using an anti-His antibody.

Production of polyclonal antisera. The 8 M urea buffer of the eluted protein was exchanged to 1 M urea by using Centriprep YM-10 columns (Millipore), according to the manufacturer's recommendations. Five mice each were immunized by using antibody multiplier (Linaris), according to the manufacturer's protocol. Totals of 0.25 mg protein/ml were dissolved in antibody multiplier S, and 0.1 ml per mouse was used for the first immunization. After 2 and 4 weeks, the mice were again immunized, with 0.1 ml protein dissolved in antibody multiplier N. Finally, after 10 weeks, the mice were sacrificed to extract the serum.

Generation of myc-tagged parasites. The complete or partial ORFs (Table 1) of the glycolytic isoenzymes, PDH subunits, and triose phosphate translocator (TPT) were amplified from the cDNA of *T. gondii* strain RH by using Phusion high-fidelity DNA polymerase (NEB) and the primers listed in Table S1 in the supplemental material. The PCR fragments were subcloned into pCR4.0-Topo (Invitrogen) or pDrive (QIAGEN), DNA sequenced, and finally cloned into AflII/AvrII- or NsiI/AvrII-digested pTetO7Sag4-acyl carrier protein (ACP)-

cmyc-dihydrofolate reductase (DHFR) vector (kindly provided by Boris Striepen), thereby replacing the ACP ORF. The final constructs consist of the anhydrotetracycline (Atc)-regulable TetO7Sag4 promoter element (35), which controls the expression of the incorporated genes with an added c-myc tag and, furthermore, includes a pyrimethamine resistance cassette for selection (6). A total of 1×10^7 parasites were electroporated with 50 μg NotI-linearized constructs as previously described (42). A total of 25 U NotI was added to the parasite suspension in the cytomix before the electroporation in order to increase the frequency of stable transfectants (3). Stably transfected parasites were selected with 1 μM pyrimethamine. The regulable TetO7Sag4 promoter would allow the generation of transgenic lines even in the case of dominant-negative effects of ectopic gene expression. The TetO7Sag4 promoter is "on" in the absence of Atc and "off" in the presence of Atc. All experiments were performed in the absence of Atc ("on"), since no negative effects of ectopic gene expression were observed.

Genome data mining and sequence comparison. Preliminary genomic and/or cDNA sequence data were accessed via http://ToxoDB.org (version 3.0) (30). Genomic data were provided by The Institute for Genomic Research (supported by NIH grant AI05093) and by the Sanger Center (Wellcome Trust). Expressed sequence tag sequences were generated by Washington University (NIH grant 1R01AI045806-01A1). Further sequences were obtained from NCBI, the *Galdieria sulfuraria* genome project website (http://genomics.msu.edu/galdieria/sequence_data.html), and the *Phaeodactylum tricornutum* website (http://genome.jgi-psf.org/Phatr2/Phatr2.home.html).

The sequences were aligned using the Clustal X program (47). The sequence alignments were subsequently inspected and edited by hand, as recommended by Harrison and Langdale (25) in order to obtain optimal alignment and eliminate gap-rich stretches. The predicted putative transmembrane-spanning regions of the plant proteins were obtained from the ARAMEMNON database (http://aramemnon.botanik.uni-koeln.de/). The transmembrane-spanning regions of the Apicomplexa were determined by using the same 16 individual prediction programs used in ARAMEMNON.

Indirect immunofluorescence assays. Samples were fixed with 4% paraformaldehyde–phosphate-buffered saline (PBS) for 10 min and permeabilized with 0.25% Triton X-100–PBS for 20 min. After being blocked for 1 h with PBS–1% bovine serum albumin (BSA), samples were incubated for 1 h with the anti-myc monoclonal antibody 9E10 (Sigma) diluted 1:250 in PBS–1% BSA, followed by incubation for 1 h with a Cy3-conjugated anti-mouse immunoglobulin G (IgG) (1:500 in PBS–1% BSA; Dianova).

Immunocytochemical staining of the tissue cysts and coccidian stages in vivo. Sections of cat small intestine containing the coccidian stages and mouse brain containing the bradyzoite stages of *T. gondii* were obtained as described previously (12). In the double-labeling immunofluorescent experiments with tissue cysts in brain, sections pretreated by pressure cooking were exposed to a mixture of mouse anti-PDH (either the E1 or E2 subunit) combined with rabbit anti-ENO1, anti-BAG1, or rat-CC2, while sections of the coccidian stages in the cat gut were exposed to mouse anti-PDH combined with either rabbit anti-ENO2 or anti-NTPase. After being washed, the sections were exposed to goat anti-mouse Ig conjugated to fluorescein isothiocyanate and goat anti-rat Ig or goat anti-rabbit Ig conjugated to Texas Red. To identify the apicoplast, semiserial sections were stained with mouse anti-enoyl reductase (ENR) and visualized by using goat anti-mouse Ig conjugated to fluorescein isothiocyanate (14) The cell nuclei were counterstained with 4,6-diamidino-2-phenylinole (DAPI) (12).

Nucleotide sequence accession numbers. Sequence data for Tg*tpiI*, Tg*tpiII*, Tg*pgkI*, Tg*pgkII*, Tg*pgmII*, Tg*pdhE1a*, and Tg*pdhE1b* have been submitted to the GenBank database under accession numbers DQ457194, DQ457193, DQ451788, DQ457189, DQ457187, DQ457185, and DQ457186, respectively. The pPT sequences have the following accession numbers: *Spinacia oleracea* TPT, CAA32016; *Brassica oleracea* TPT, U13632; *Arabidopsis thaliana* glucose-6-phosphate translocator (GPT), At5g54800; *Galdieria sulfuraria* PT I, Contig09803.g31.t1; *Phaeodactylum tricornutum* PT I, Phatr2¦8738¦e_gw1.1.362.1; *P. tricornutum* PT II, Phatr2¦9889¦e_gw1.2.246.1; *P. falciparum* TP I, NP_703643; *P. falciparum* TP II, NP_703428; *Plasmodium berghei* PT I, CAH95951; *P. berghei* PT2, CAH94954; *Plasmodium chabaudii* PT, CAH76867; *Plasmodium yoelii* PT I, EAA21183; *P. yoelii* PT II, EAA15460; TgPT, 55.m10326; *Babesia bovis* PT, ABC25608; *Theileria parva* PT, EAN31281; and *Theileria annulata* PT, XP_955232.

RESULTS

Identification of multiple glycolytic isoenzymes in the *T. gondii* genome. In order to identify the complete set of *T. gondii* genes which encode the glycolytic enzymes, we used the amino acid sequences of all the glycolytic enzymes from *Plasmodium falciparum*, *Saccharomyces cerevisiae*, *Arabidopsis thaliana*, and *Homo sapiens* for a BLASTP search in the *T. gondii* database ToxoDB (30). The 10 enzymes that typically form the glycolytic pathway were predicted to be present in *T. gondii.* With the exception of hexokinase and glucose-6-phosphate isomerase (GPI), which are encoded only once in the genome, the remaining eight enzymes, from phosphofructokinase up to pyruvate kinase (PK), are encoded by two genes (Table 1). The tandemly linked localization of the two genes encoding isoforms of fructose bisphosphate aldolase on chromosome X and their high overall sequence similarity at the DNA level of 82% suggest that both genes arose from a gene duplication of an ancestral gene.

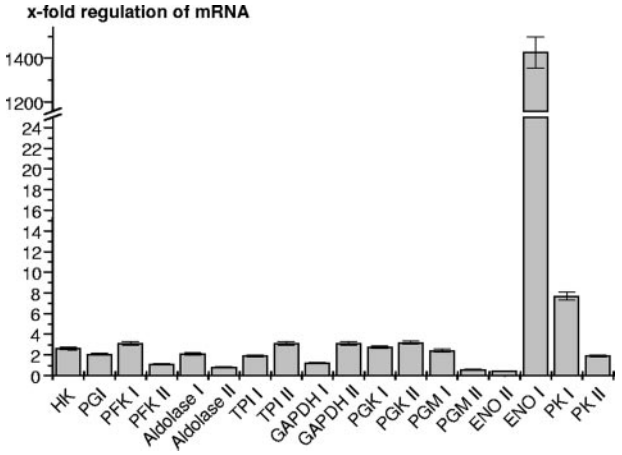

FIG. 1. Comparison of the mRNA expression levels of glycolytic genes between tachyzoites and bradyzoites. Light-cycler PCR (Roche) was performed to amplify cDNAs from tachyzoites and in vitro bradyzoites by using primer pairs for all 18 glycolytic genes identified in the *T. gondii* genome. For abbreviations of the amplified genes, see Fig. 2B. The values represent the mRNA ratios for bradyzoites/tachyzoites for each gene after normalization for actin expression. The means ± standard deviations of the results from triplicate experiments are given. Only the mRNA expression for the known bradyzoite marker ENO1 is strictly stage-specifically regulated. PK I is induced eightfold in bradyzoites, while all other genes display less than a fourfold difference in mRNA expression levels between tachyzoites and bradyzoites.

mRNA expression of glycolytic genes in tachyzoites versus in vitro bradyzoites. The two ENO genes were recently shown to be stage-specifically regulated at the mRNA level (8). We thus investigated whether stage-specific mRNA regulation also occurs in the isoforms of the other glycolytic genes. The transcript levels of the complete set of 18 genes encoding the glycolytic enzymes were compared between the tachyzoites and in vitro bradyzoites by light-cycler real-time RT-PCR (Fig. 1). These in vitro bradyzoites are immature and, in contrast to tissue cyst-derived bradyzoites, have just started, but not completed, their development. A strong upregulation in the in vitro bradyzoites was found only for ENO1 (1,450-fold). The PK I displayed a moderately (eightfold) elevated mRNA level in the bradyzoites. All the remaining isoforms showed less-than-fourfold differences in their mRNA levels between the tachyzoites and bradyzoites.

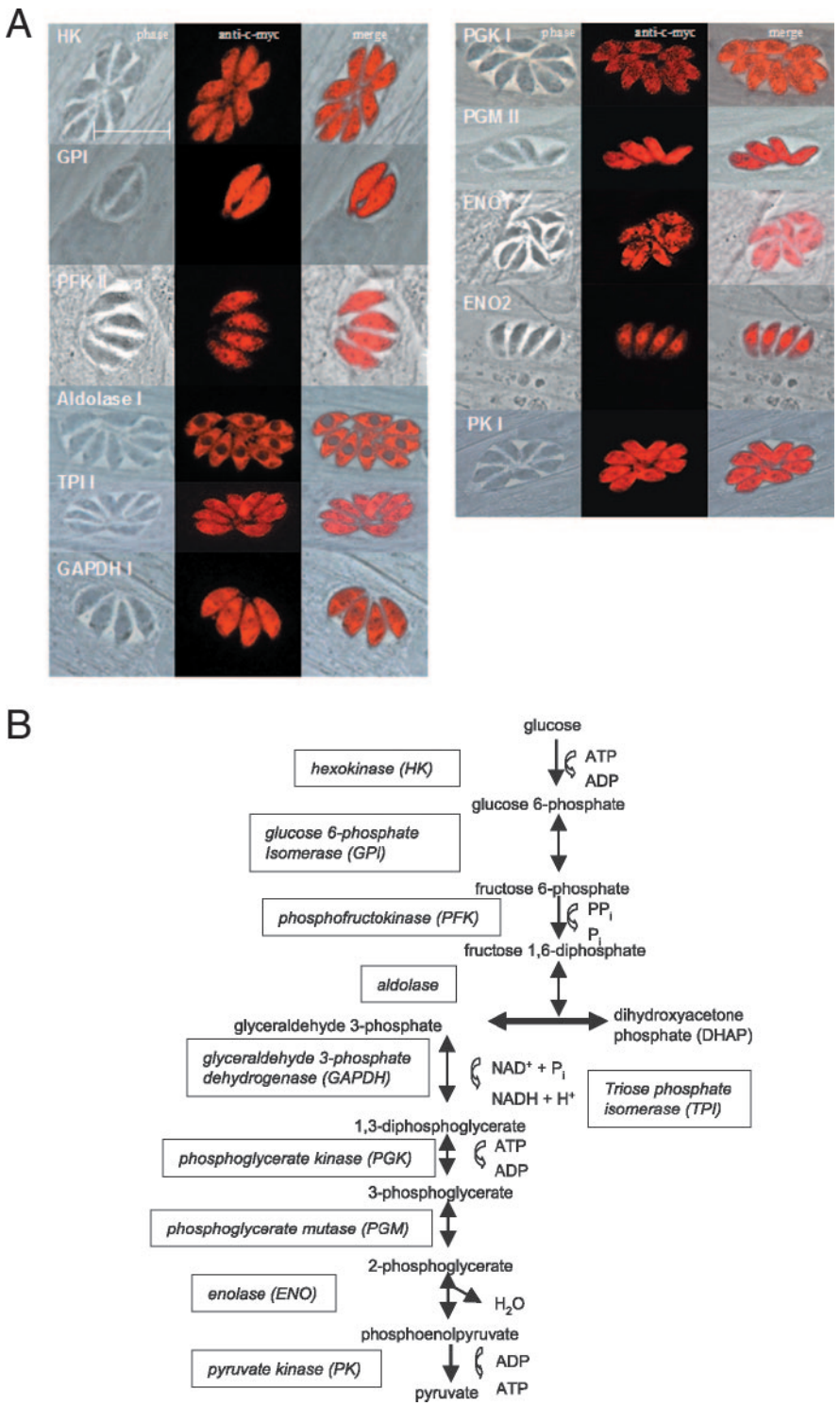

FIG. 2. A complete set of glycolytic enzymes is targeted to the cytosol. (A) RH TATi parasites were electroporated with expression plasmids which contain the ORFs of the indicated genes fused to a C-terminally located c-myc tag. The complete ORFs of the indicated genes were expressed, with the exception of phosphofructokinase I, for which only the first 500 amino acids were used. The fusion proteins were detected in stably transfected parasites by indirect immunofluorescence staining using an anti-myc antibody. (B) All the enzymes necessary for a typical glycolytic pathway are targeted to the cytosol of *T. gondii*. All images are at the same magnification. The bar represents 10 μm.

Localization of glycolytic isoenzymes. Since plant plastids are well known to contain various glycolytic isoenzymes, it was of interest to investigate whether some of the *T. gondii* isoforms are targeted to the apicoplast. A commonly found structure of nucleus-encoded apicomplexan proteins which mediates targeting to the apicoplast is an N-terminally located bipartite signaling sequence which is composed of a signal peptide and a transit peptide of various lengths (48). When

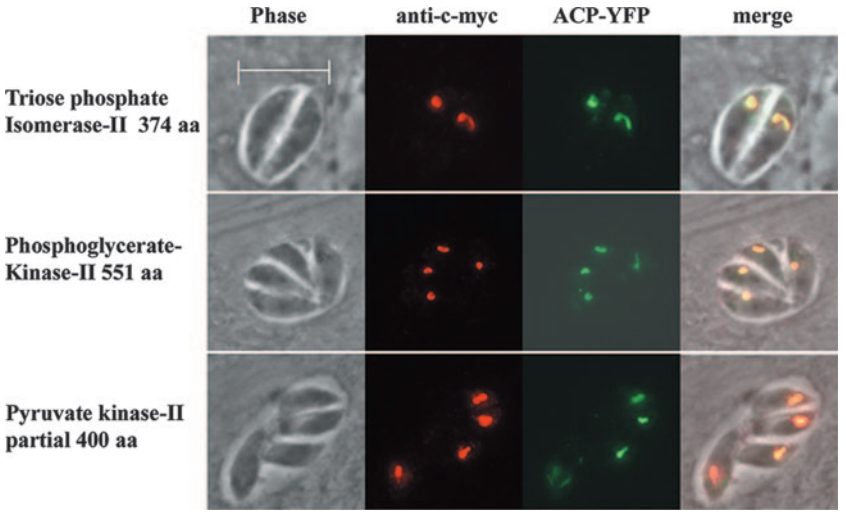

FIG. 3. TPI II, PGK II, and PK II are targeted to the apicoplast. RH TATi parasites were stably tranfected with expression plasmids which contained the ORFs of the indicated genes fused to a C-terminally located c-myc tag. For TPI II and PGK II, the complete ORF of the indicated length was expressed. For PK II, the first 400 amino acids (aa) were used. Stably transfected parasites were subjected to a second transfection with pSag-ACP-YFP Cat, which encodes the apicoplast marker protein ACP-YFP. The myc-tagged fusion proteins were detected by indirect immunofluorescence staining using an anti-myc antibody. The obtained signals colocalize with the ACP-YFP signal, thus confirming the plastid localization. All images are at the same magnification. The bar represents 10 μm.

analyzed with the SignalP algorithm (1), the three glycolytic enzymes triose phosphate isomerase II (TPI II), glyceraldehyde-3-phosphate dehydrogenase II (GAPDH II), and phosphoglycerate kinase II (PGK II) are predicted to contain an N-terminal signal sequence (Table 1) which is followed by a putative transit peptide that is composed of several positively charged amino acids at the N terminus. These enzymes are thus putative candidates for an apicoplast localization. The SignalP algorithm predicts a signal anchor for PK II, while neither a signal peptide nor a signal anchor was predicted for the remaining glycolytic enzymes. Since there are also proteins, such as one of the *Plasmodium* pPTs (PfoTPT), which lack the N-terminal bipartite sequence but are nevertheless targeted to the apicoplast, an experimental confirmation of the predicted localizations is important.

To gain experimental evidence of the localization for the *T. gondii* glycolytic isoforms, we investigated their targeting by epitope tagging experiments. RH strain parasites of the TATi-1 line were transfected with expression plasmids (pTetO7Sag4-candidate gene-cmyc-DHFR) which contained the ORF of the candidate gene fused to a C-terminally located c-myc tag. The promoter for these plasmids allowed tetracycline-regulated transgene expression in the TATi line (35). For the majority of analyzed genes, the complete ORF was used for the expression analysis. PCR amplification of the complete ORF failed for phosphofructokinase II and PK II, and we thus used truncated versions of these genes of 500 and 400 amino acids for cloning. While truncated fusion proteins should be faithfully targeted to the apicoplast when the N terminus contains the targeting signal, a potential risk of mistargeting exists when internal sequences mediate the targeting. The final expression plasmids were subjected to DNA sequencing in order to confirm the integrity of the ORFs. DNA sequences are given in the supplemental material (Fig. S3).

We excluded four genes, namely, the GAPDH II, phosphofructokinase I, fructose-bisphosphate aldolase II, and phosphoglycerate mutase I (PGM I) genes, from further analysis. For GAPDH II and phosphofructokinase I, the initiation start codon could not be clearly identified, and for fructose-bisphosphate aldolase II and PGM I, the ORFs were found to be interrupted by stop codons, even after repeated PCR cloning. However, a comparison of the sequences with expressed sequence tags in ToxoDB revealed that transcripts for the latter two genes exist which do not contain these stop codons. Although the reason for the failure of ORF amplification remains unclear, there is thus no evidence of fructose-bisphosphate aldolase II and PGM I being encoded by pseudogenes.

The localization of the remaining 14 glycolytic proteins was analyzed in stably transfected parasite populations by indirect immunofluorescence microscopy using an anti-myc antibody. A complete set of all 10 enzymes which form the glycolytic pathway was found to be targeted to the cytosol, indicating that this pathway is indeed present in this compartment (Fig. 2A and B). For the tachyzoite-specific ENO2, strong labeling was found in the nucleus, with weaker labeling in the cytosol. Three isoforms, namely, TPI II, PGK II, and PK II, localized to a parasite structure which has the typical shape and location of the apicoplast (Fig. 3). The plastid localization was confirmed by colocalization studies in parasites which were transfected with a plasmid (pSag-ACP-YFP Cat; kindly provided by B. Striepen) encoding an apicoplast marker protein (33, 49).

The native PDH complex is exclusively expressed in the apicoplast. The PDH complex is composed of the four subunits E1-alpha, E1-beta, E2, and E3. Plant genomes typically possess two gene copies for each subunit, which encode a mitochondrial and a plastid PDH complex, respectively. The genome of *T. gondii* is similar to the *Plasmodium* genome in containing two genes encoding E3 subunits but has only single-copy genes for E1-alpha, E1-beta, and E2 (20). N-terminal parts of the plasmodium E1-alpha and E2 subunits and the *T.*

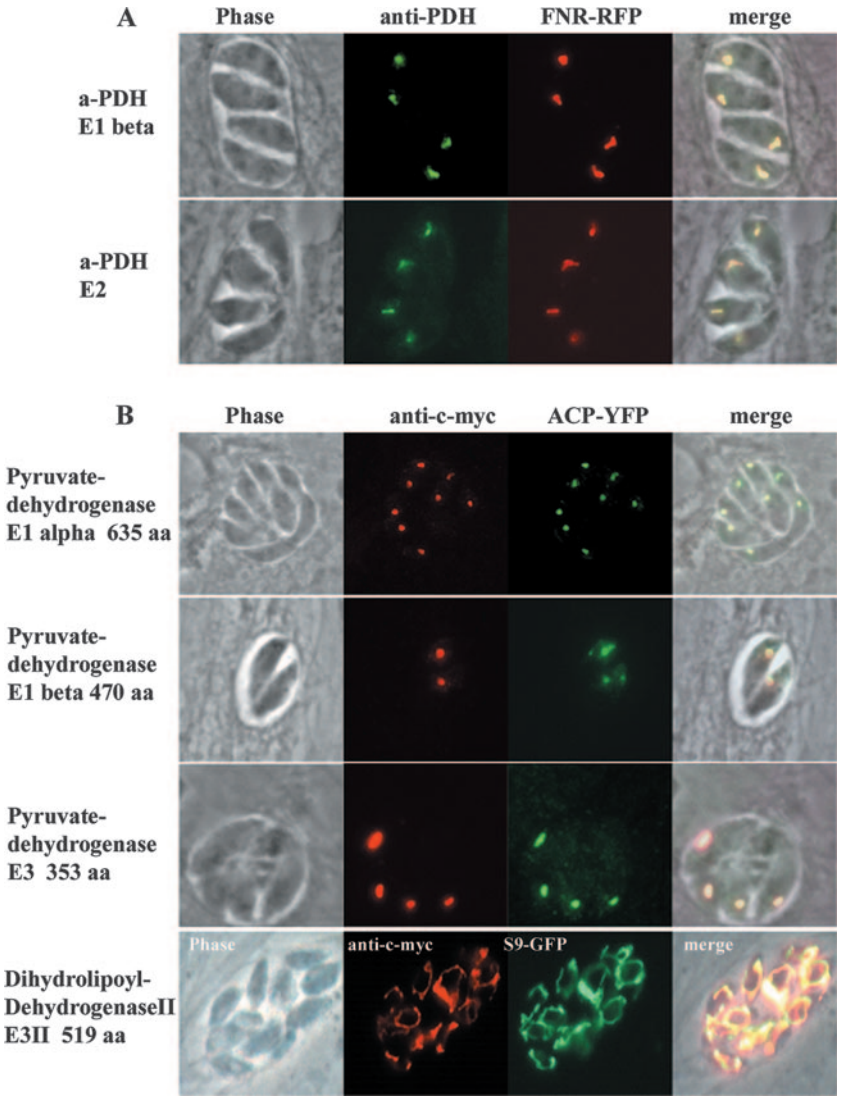

FIG. 4. All four PDH subunits are localized inside the apicoplast. (A) Localization by epitope tagging. The complete ORFs of the E1-alpha, E1-beta, E3 I, and E3 II subunits were cloned in frame to a C-terminally localized c-myc tag, and the plasmids were stably transfected into RH TATi parasites. Plastid localization was confirmed by colocalization with an ACP-YFP fusion protein. The mitochondrial localization of dihydrolipoyl-dehydrogenase II/E3 II was confirmed by colocalization using the mitochondrial marker S9-GFP (5). (B) Polyclonal mouse antisera against the PDH E1 beta and E2 subunits were used to confirm the plastid localization of the PDH complex. The plastid localization was confirmed by colocalization with an FNR-RFP fusion protein. All images are at the same magnification. The bar represents 10 μm. aa, amino acids.

gondii E2 subunits were previously fused with green fluorescent protein (GFP) or yellow FP (YFP) and were shown to be targeted to the apicoplast (4, 20). To confirm the plastid localization of the PDH complex on the level of the native protein, we raised antisera against purified *T. gondii* E1-beta and E2 subunits which had been recombinantly expressed in *E. coli*. The antisera were used for immunofluorescence staining of cells, which were stably transfected with the apicoplast marker ferredoxin-$NADP^+$-reductase (FNR)–red FP (RFP) (33). The colocalization of the obtained fluorescence signals confirmed that the E1-beta and E2 subunits are solely targeted to the apicoplast (Fig. 4A), without any signal for the mitochondrion.

In addition, we performed epitope tagging experiments on full-length proteins, as described above. Strain RH parasites of the TATi-1 line were transfected with expression plasmids (pTetO7Sag4-candidate gene-cmyc-DHFR) which contained the ORFs of the E1-alpha, E1-beta, and both E3 subunits fused to a C-terminally located c-myc tag. Immunofluorescence analysis of stably transfected parasite populations revealed that E1-alpha, E1-beta, and E3 I are exclusively localized to the apicoplast, with no labeling of the single mitochondrion (Fig. 4B). The apicoplast targeting was confirmed by colocalization experiments using the apicoplast marker ACP-YFP. The second E3 subunit (dihydrolipoyl-dehydrogenase II/E3 II) was targeted to the single mitochondrion, as demonstrated by colocalization studies (Fig. 4B) using the mitochondrial marker S9-GFP (5).

In vivo expression and location of PDH in brain tissue cysts and cat gut stages. The antisera against the E1-beta and E2 subunits were used to examine the expression levels of the

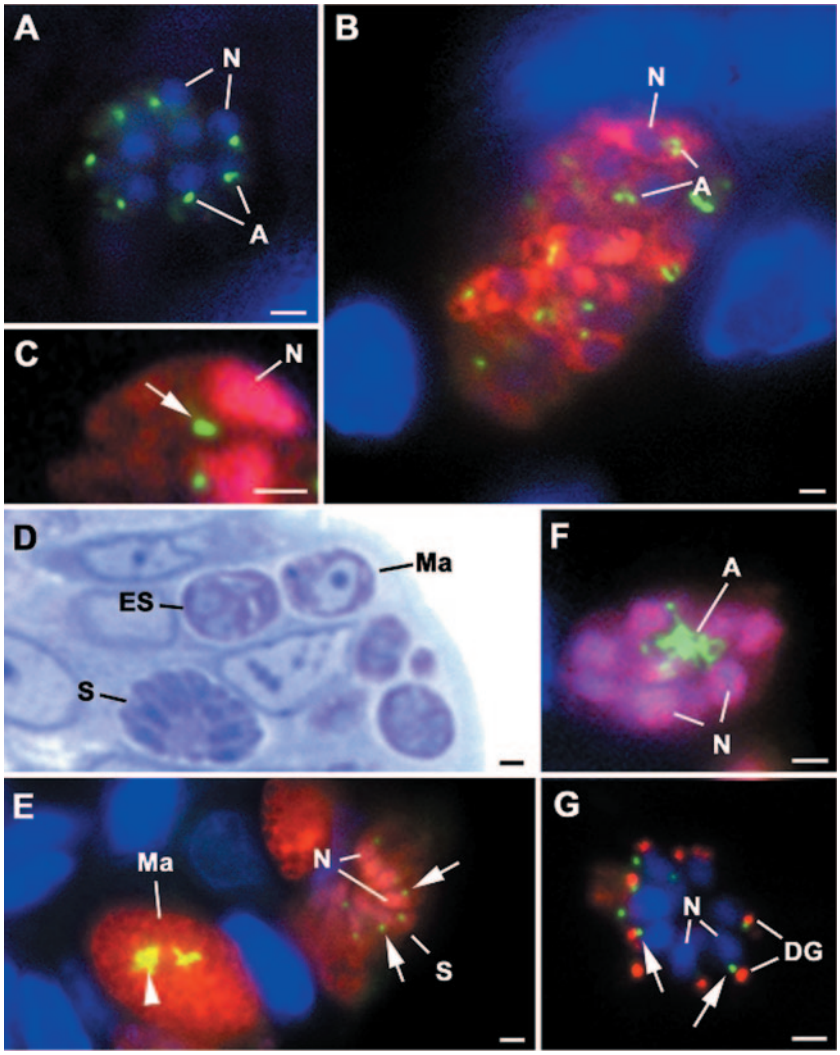

FIG. 5. The PDH complex is expressed during the tissue cyst formation and coccidian development of *T. gondii*. (A) Section through a lesion in the brain showing stage conversion with a rosette of BAG1-negative tachyzoites showing a single small PDH^+ structure (A, green) just anterior to the nucleus (N). The tachyzoites were stained with anti-PDH and anti-BAG1. The bar is 1 μm. (B) Section through an early tissue cyst from the same section as the image in panel A. The tissue cyst contains numerous $BAG1^+$ (red) bradyzoites showing slightly elongated apicoplasts (A) labeled with ant-PDH E1-beta (green) adjacent to the nuclei (N). The bar represents 1 μm. (C) Detail of a bradyzoite showing a tissue cyst double labeled with anti-PDH (green) and anti-ENO1 (red) showing low-level cytoplasmic and intense nuclear (N) staining for ENO1. Note the PDH^+ structure adjacent to the nucleus (arrow). The bar represents 1 μm. (D) Low-power micrograph through part of a villus of an infected cat showing various developmental stages. The section is a 1-μm plastic-embedded section showing the morphological features of the early (ES) and mature (S) schizonts and the macrogametocyte (Ma). The section is stained with azure A. The bar represents 1 μm. (E) An immunostained section of an area similar to that in panel D double labeled with anti-PDH (green) and anti-ENO2 (red) was single labeled with anti-PDH E2 (green), showing the intensely labeled apicoplasts (arrowhead) associated with the macrogametocytes (Ma) and smaller structures (arrows) associated with the nuclei (N) of the merozoites in the mature schizonts (S). The bar represents 1 μm. (F) Detail of an early multinucleate (N) schizont double labeled with anti-PDH (green) and anti-ENO1 (red), showing a complex elongated apicoplast (A) within the cytoplasm strongly labeled with anti-PDH E2 (green). The bar represents 1 μm. (G) A mature schizont double labeled with anti-PDH (green) and anti-NTPase (red) in which the fully formed merozoites possess a single small PDH^+ structure (arrows) in the apical cytoplasm between the nucleus (N) and the dense granules (DG) positively labeled with anti-NTPase. The bar represents 1 μm.

PDH complex in various developmental (differentiation) stages of the parasite. Tachyzoites, characterized as being BAG1 negative, in lesions showing stage conversion in the brain exhibited a single small spherical structure just anterior to the nucleus, similar to that observed in vitro (Fig. 5A). In both early and mature tissue cysts, the bradyzoites, characterized as BAG1 positive, also showed small perinuclear structures positively stained with anti-PDH, which in certain cases appeared slightly elongated or duplicated (Fig. 5B and C) This appearance is similar to that seen when bradyzoites were stained with anti-ENR (14) and would be consistent with PDH being located within the apicoplast. In sections of the small intestine of a cat containing both the asexual and sexual coccidian stages (Fig. 5D), it was observed that there were variations in the staining intensities and shapes of the structures labeled with anti-PDH that appeared to relate to morpholog-

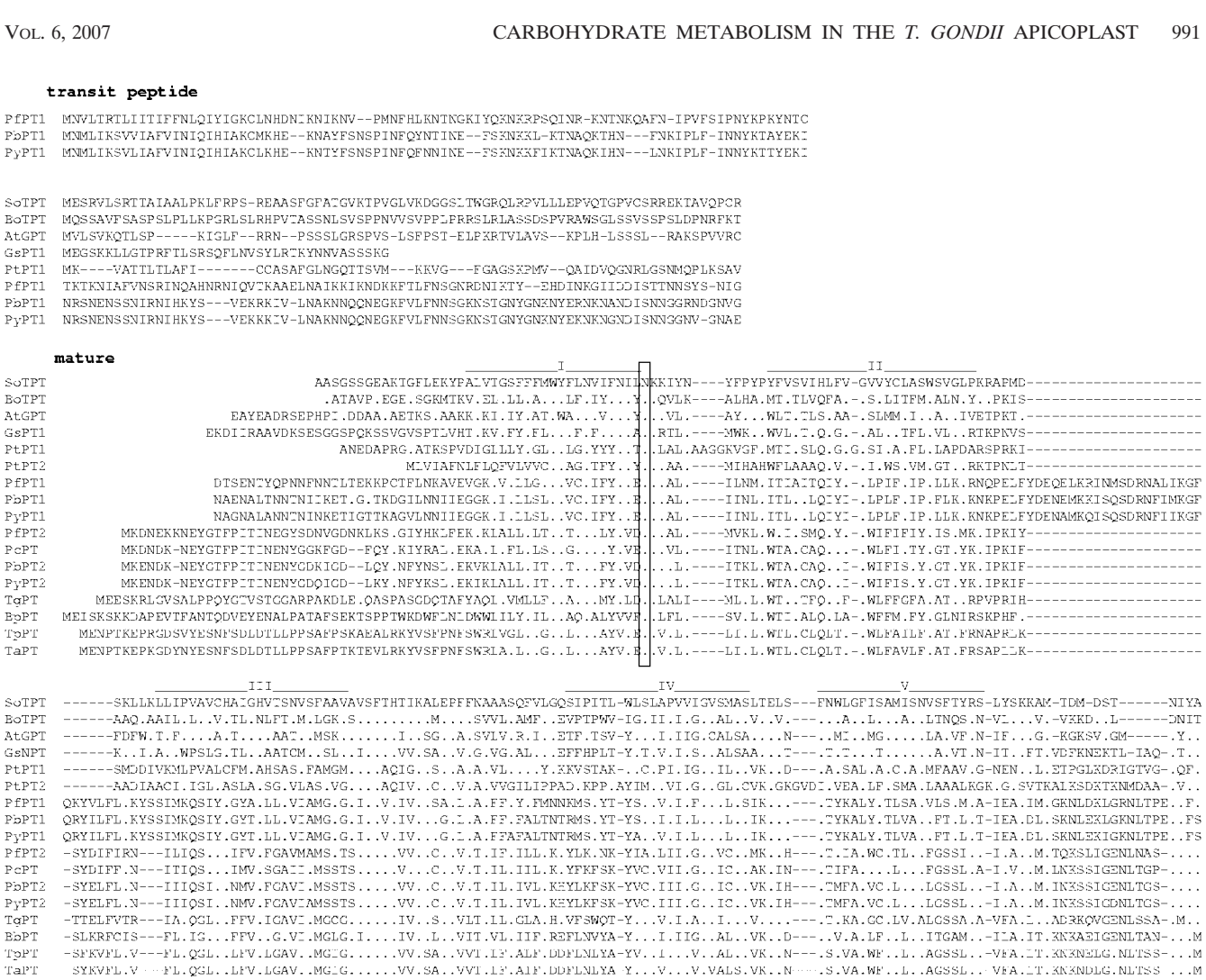

FIG. 6. Sequence comparison of pPTs from higher plants, algae, and Apicomplexa. Sequences were obtained from NCBI, the *Galdieria sulfuraria* genome project website (http://genomics.msu.edu/galdieria/sequence_data.html), the *Phaeodactylum tricornutum* website (http://genome.jgi-psf.org/Phatr2/Phatr2.home.html), and the *Toxoplasma gondii* database ToxoDB. The TPT sequence from spinach (*Spinacia oleracea*) was aligned with the following sequences: the TPT from *Brassica oleracea*, the GPT from *Arabidopsis thaliana*, a pPT from *Galdieria sulfuraria*, two pPTs from *Phaeodactylum tricornutum*, two pPTs from *Plasmodium falciparum*, two pPTs from *P. berghei*, a pPT from *P. chabaudii*, pPTs from *P. yoelii*, a pPT from *Toxoplasma gondii* (TgPT), a pPT from *Babesia bovis*, a pPT from *Theileria parva*, and a pPT from *T. annulata*. The sequence comparison and prediction of transmembrane helices were done as described in Materials and Methods. The identities of amino acid residues to the *Spinacia oleracea* TPT sequence are indicated by dots. The locations of transmembrane helices are indicated by solid lines, while two potential substrate binding sites are marked by boxes.

ical changes associated with parasite development (Fig. 5E). In sections double labeled with anti-PDH and anti-ENO1, during the early proliferative phase of asexual development (endopolygeny), the PDH was associated with a strongly staining elongated or branched structure, while the nuclei were strongly stained and the cytoplasm was lightly stained for ENO1 (Fig. 5E). In fully formed merozoites of the mature schizonts, a single small lower-intensity-stained structure was observed in

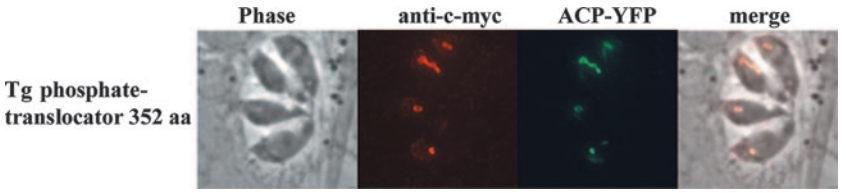

FIG. 7. Plastid localization of the TgPT. The complete ORF of the TgPT was cloned in frame to a C-terminally localized c-myc tag and stably transfected into RH TATi parasites. The plastid localization was confirmed by colocalization with an ACP-YFP fusion protein. All images are at the same magnification. The bar represents 10 μm. aa, amino acids.

the apical cytoplasm adjacent to the nuclei (Fig. 5E) and posterior to the dense granules identified by positive staining for NTPase (Fig. 5G). In the developing microgametocyte, only the small low-intensity-stained structure was observed (not shown). In contrast, within the developing macrogametocyte, a large lobated structure was strongly stained for PDH, while the cytoplasm was positively stained for ENO1 (Fig. 5E). These staining patterns were similar to those observed in sections stained with the apicoplast marker ENR (14). The results were consistent with PDH being located within the apicoplast during the various developmental stages and show changes in organellar shape and staining intensity similar to those observed for ENR.

The *T. gondii* phosphate translocator (TgPT). Phosphorylated intermediates of glycolysis, like glucose-6-phosphate, triose phosphates, and phosphoenolpyruvate (PEP), are transported by a family of pPTs. Recently, two proteins with significant homologies to plant pPTs have been described in *Plasmodium falciparum* (36). While one protein, with a bipartite targeting sequence (PfiTPT), is located in the innermost envelope membrane, the other protein (PfoTPT), lacking a cleavable targeting peptide, is located in the outermost envelope membrane. To identify PTs in *Toxoplasma* and other Apicomplexa members, BLAST searches against entries in GenBank were conducted. These searches revealed that other *Plasmodium* species also possess two pPTs with high similarities to PfiTPT and PfoTPT, respectively (Fig. 6). In contrast, the Apicomplexa-like *Babesia bovis* and *Toxoplasma* and *Theileria* species possess only one pPT, each of which shows high sequence similarity to PfoTPT and which also lack N-terminal targeting sequences. Interestingly, red algae, such as *Phaedactylum* and *Galdieria*, also possess two different pPTs, one having an N-terminal extension and one lacking it (Fig. 6). A specific feature of the PfiTPT of the *Plasmodium* species which has not been found in any other pPTs so far is an insertion of 22 amino acids between membrane-spanning regions 2 and 3.

To determine the subcellular localization of the TgPT by epitope tag expression, the complete ORF of the pPT was cloned into an expression plasmid (pTetO7Sag4-candidate gene-cmyc-DHFR) and the final construct was transfected into RH strain parasites of the TATi-1 line. Immunofluorescence analysis was performed on stably transfected parasite populations, which were cotransfected with the apicoplast marker ACP-YFP. The immunofluorescence signals were weaker and the staining pattern was more heterogeneous than for the other localized proteins in this study. The fluorescence signal for most of the positively stained parasites colocalized with the apicoplast marker (Fig. 7). However, in some parasites, a reticular staining pattern was observed which appeared to be outside of the apicoplast.

DISCUSSION

Carbohydrate metabolism plays a central role in energy production and the synthesis of metabolites in all cells. To obtain additional insights into the metabolism of *T. gondii*, we analyzed several key enzymes of carbohydrate metabolism and showed that they localize either to the apicoplast or the cytosol.

Toxoplasma possesses a single PDH complex, which is localized in the apicoplast and is absent from the mitochondrion. The apicoplast targeting was demonstrated for the two subunits E1-beta and E2 by immunolocalization of the native protein using antisera generated against recombinant proteins. Furthermore, for the three PDH subunits E1-alpha, E1-beta, and E3 I, the apicoplastic localization was also shown by the expression levels and immunolocalization of myc-tagged full-length fusion proteins. Our results confirm those of previous studies, in which truncated fusions of *P. falciparum* E1-alpha and E2 with GFP and a truncated *T. gondii* E2 fusion with YFP were shown to be targeted to the apicoplast (4, 20). We found the second *T. gondii* PDH E3 subunit to be localized to the mitochondrion and absent from the apicoplast. However, as in *Plasmodium*, this subunit is most likely part of the α-ketoglutarate dehydrogenase and the branched-chain ketoglutarate dehydrogenase complex present within the mitochondrion (20, 34). With the aid of the recombinant antisera, PDH expression was detected in all stages of *T. gondii*, including tachyzoites, in vitro-induced early bradyzoites, mature bradyzoites within tissue cysts, and both the asexual and sexual coccidian stages in the cat gut.

The absence of the PDH complex from mitochondria and its presence in apicoplasts has important implications for acetyl-CoA-dependent pathways. Acetyl-CoA is required in the apicoplast for type II fatty acid synthesis, which takes place in this compartment and was shown to be essential for the parasite (33). The first step in fatty acid synthesis is catalyzed by an acetyl-CoA carboxylase, which was recently shown to be targeted to the apicoplast (26). Acetyl-CoA could be derived from three different sources, namely, from pyruvate, acetate, or citrate (38). In plants, the actual source of acetyl-CoA is still controversial and might depend on the species, the developmental stage, the plant tissue, and the type of plastid (17).

Acetate enters plant plastids, and probably also apicoplasts, by diffusion through the lipid bilayer (17, 37) and is then converted to acetyl-CoA by acetyl-CoA synthetase, which in

plants is located in the plastids (44). However, although an acetyl-CoA synthetase is predicted in the *T. gondii* genome, the coding sequence lacks a signal sequence and the enzyme is thus most likely localized in the cytosol (22); i.e., it might be involved in the provision of cytosolic acetyl-CoA. In plants, citrate is split into oxaloacetate and acetyl-CoA by ATP:citrate lyases located in the cytosol and/or in plastids (11, 41). The *T. gondii* genome contains a single ATP:citrate lyase gene, which, as the acetyl-CoA synthetase lacks a signal peptide and a signal anchor, is thus most likely not targeted to the apicoplast. Thus, the PDH complex appears to be the only enzyme which can provide the apicoplast with acetyl-CoA, which means that plastid acetyl-CoA is mainly if not exclusively derived from pyruvate.

In an attempt to obtain further insight into carbohydrate metabolism in Apicomplexa, we looked for the genes encoding all the glycolytic enzymes in *T. gondii*. We identified the genes encoding all the enzymes that are necessary for the conversion of glucose into pyruvate. In addition, we could demonstrate by using myc-tagged fusion proteins that the cytosol of *T. gondii* contains a complete set of enzymes for glycolysis, starting from hexokinase and ending with PK (Fig. 2). These enzymes should allow the parasite to metabolize glucose into pyruvate, the product of glycolysis, which is located in the cytosol of almost all organisms.

During the *T. gondii* stage differentiation, regulation of the carbohydrate metabolism is likely to occur, since amylopectin granules are acquired during tachyzoite-to-bradyzoite differentiation and are degraded during the bradyzoite-to-tachyzoite transition (7). Our relative quantification of the mRNA levels for the complete set of glycolytic genes in tachyzoites and in vitro-induced (immature) bradyzoites revealed that, in the early phase of stage differentiation, only ENO1 displayed a strong (1,450-fold) induction. All other glycolytic genes revealed minor or moderate levels of regulation, between 0.4-fold (ENO2) and 8-fold (PK I). In early bradyzoites, a strong upregulation of glycolytic genes is thus restricted to ENO1, which was shown before to be induced in bradyzoites (53). Since the mRNA from our in vitro-induced bradyzoites is not free from tachyzoite-specific transcripts, we cannot exclude that mRNA levels in mature, tissue cyst-derived bradyzoites are different. Furthermore, the regulation of carbohydrate metabolism during differentiation might also occur at levels other than mRNA amounts, for example, protein stability or enzymatic activity.

Remarkably, all glycolytic enzymes, from phosphofructokinase up to PK, are present in the *T. gondii* genome as duplicates. By using myc-tagged fusion proteins, we could localize the isoforms of TPI II, PGK II, and PK II in the apicoplast. We obtained for the tachyzoite-specific ENO, ENO2, a stronger signal in the nucleus than in the cytosol, which is in agreement with the results of a recent study in which both ENO isoforms were localized by using specific antisera (13). Ferguson et al. (13) also localized the bradyzoite-specific ENO, ENO1, predominantly to the nucleus, while the myc-tagged copy of our transfected parasites was predominantly localized in the cytosol. A putative explanation for this discrepancy is the misexpression of the bradyzoite-specific ENO1 in the tachyzoite stage in our epitope tag experiments, which might prevent correct nuclear transportation, possibly due to the lack of an appropriate import machinery in the tachyzoite stage.

GAPDH II was very recently localized to the apicoplast (D. Soldati, personal communication). The location of the remaining isoforms of the glycolytic enzymes, namely, phosphofructokinase I, aldolase II, and PGM II, remains to be experimentally confirmed. The absence of ENO activity in the apicoplast means that, even if a PGM which converts 3-phosphoglycerate (PGA) into 2-PGA is present in the apicoplast, further conversion of TPs into pyruvate does not occur in this compartment, but is restricted to the cytosol. This metabolic situation is comparable to that of most types of plant plastids, which also possess an additional, but incomplete, glycolytic pathway, in that glycolysis cannot proceed further than to 3-PGA, due to the absence (or very low activities) of PGM and/or ENO (17).

The role of PTs. In plants, both glycolytic pathways are connected with each other by pPTs that transport phosphorylated intermediates of glycolysis across the inner envelope membrane (18). *Arabidopsis* possesses six pPTs, which can be split into four different subfamilies according to their overall sequence identities, gene structures, and substrate specificities (31). The TPT exports triose phosphates from chloroplasts in exchange for inorganic phosphate or 3-PGA, while the pPT and the GPT import PEP and glucose-6-phosphate, respectively, into plastids (16, 28). The fourth pPT, the xylulose PT, transports xylulose-5-phosphate across the inner envelope membrane, but has been found so far only in *Arabidopsis* (9). Mullin and coworkers (36) identified two PTs in *Plasmodium falciparum* with homologies to plant pPTs. Because the proteins are located in the inner (PfiTPT) and outermost (PfoTPT) envelope membrane of the apicoplast, these authors proposed that they act in tandem to transport phosporylated compounds into the plastid. While other *Plasmodium* species also possess two pPTs, we, surprisingly, found only one pPT for other apicomplexan parasites, such as *Toxoplasma*, *Theileria*, and *Babesia*. However, because the genome of *Babesia* is not fully sequenced, the presence of a second pPT could not be excluded. All of these proteins resembled the pPT of the outermost membrane. The absence of a second pPT in these organisms could be explained in different ways. (i) The transport of metabolites across the innermost membrane in these species is completely different from that in *Plasmodium*. (ii) The pPT in *Toxoplasma* and other Apicomplexa is targeted not only to the outermost membrane, but also to the other envelope membranes, although it does not contain a bipartite N-terminal targeting sequence. Dually targeted proteins are commonly found in eukaryotic cells (45), including proteins that are targeted to envelopes and thylakoid membranes in chloroplasts, while dual targeting to the different envelope membranes has not been shown in plants. Strikingly, very recently, the localization of the TgPT to different envelope membranes has been shown by immunogold labeling, although it was not possible to definitively state that the protein is present in all four membranes (29). Thus, it is reasonable to assume that the TgPT transports glycolytic intermediates not only across the outermost but also across some of the other envelope membranes.

The same group showed that the localization of the pPT varied throughout the cell cycle. Early-stage parasites showed a circumplastid distribution, whereas at a later stage, the signal

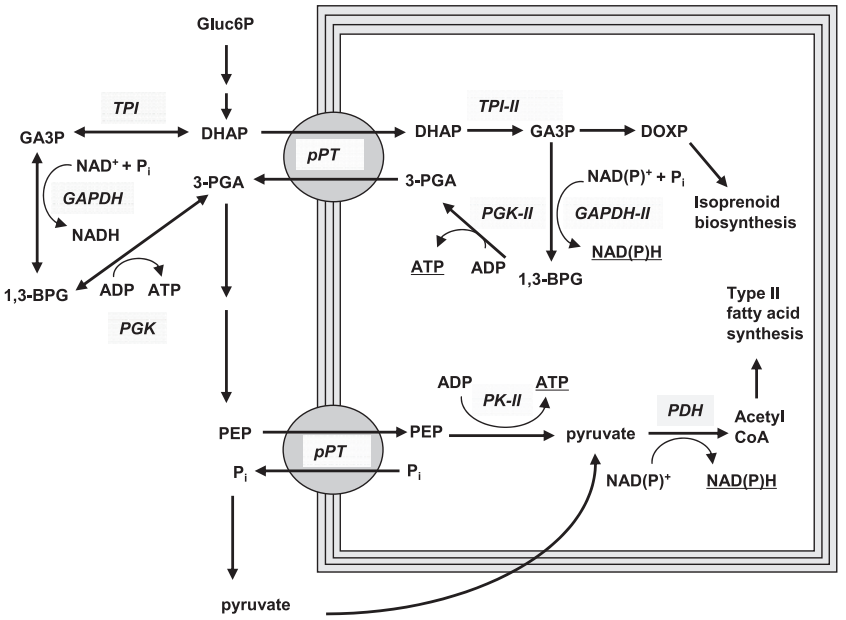

FIG. 8. Putative pathways for import of carbon into the apicoplast and generation of ATP and reduction power for fatty acid synthesis. The triose phosphate DHAP is transported from the cytosol into the apicoplast by the pPT and converted into 3-PGA by the action of TPI II, a putative apicoplastidic GAPDH II, and PGK II. The relocation of these central glycolytic reactions into the apicoplast would lead to a net transfer of ATP (via PGK II) and the reduction power (via GAPDH II) from the cytosol to the apicoplast. 3-PGA is proposed to leave the apicoplast via the PT and is, in the cytosol, either converted back into DHAP, thereby forming a reverse triose phosphate–3-PGA shuttle, or converted into PEP and pyruvate, which are then reimported into the apicoplast by the pPT or by a so-far-unknown plastid pyruvate transporter. Inside the apicoplast, PEP and ADP can be converted by PK into pyruvate and ATP.

was detected in vesicles adjacent to the plastid. This cell cycle-specific distribution might explain the heterogeneous staining pattern which we observed in parasites which were transfected with the epitope-tagged pPT. It has been proposed that the function of these vesicles is to convey TgPT to the apicoplast by fusion with the outermost membrane (29).

An important parameter for the metabolic fluxes within the apicoplast is certainly the substrate specificity of the TgPT. For example, the sources of carbon and reducing equivalents (NADPH) for fatty acid synthesis are at present unknown. Unfortunately, the substrate specificity of the TgPT cannot simply be deduced from its amino acid sequence or putative substrate binding site, because the pPTs from the Apicomplexa, and also from algae such as *Galdieria* and *Phaeodactylum*, do not show particularly high similarities to one of the four subfamilies of higher plant pPTs (for an extensive discussion of the putative substrate binding sites, see reference 31). If glucose-6-phosphate is imported into the plastid, it cannot enter the glycolytic pathway, since we have shown that *T. gondii* has only one GPI, which is located in the cytosol.

Based on the data presented here and on recently published data on *Toxoplasma* and *Plasmodium* plastid proteins, we propose the following model for the supply of carbon and reducing equivalents to the apicoplasts (Fig. 8). The PT imports the triose phosphates dihydroxyacetone phosphate (DHAP) and GAP into the apicoplasts. GAP has two functions in the apicoplasts. First, it serves as a substrate for the deoxyxylulose-5-phosphate pathway, which is located in the apicoplast (27) and which leads to the synthesis of several isoprenoids. Second, it could be converted by GAPDH to 1,3-bisphosphoglycerate. Based on the presence of a leader peptide and a bipartite signaling sequence, the second GAPDH isoform was recently proposed to be targeted to the apicoplast (10). 1,3-Bisphosphoglycerate is then metabolized by PGK to 3-PGA (Fig. 8).

With cytosolic and plastid isoforms of PGK, GAPDH, and TPI, along with a TPT, all components are expressed in *T. gondii*, which would form a reverse triose phosphate–3-PGA shuttle (Fig. 8). This shuttle transfers triose phosphates from the cytosol to the apicoplast in exchange for 3-PGA and thus results in a net transfer of ATP and reduction power from the cytosol to the apicoplast. Both are needed for its biosynthetic pathways, e.g., for fatty acid synthesis, and could explain the lack of other obvious pathways for energy production in this organelle.

On the other hand, 3-PGA could be converted to PEP and pyruvate in the cytosol, which are then reimported into the apicoplast by the pPT or by a so-far-unknown plastid pyruvate transporter. Inside the apicoplast, PEP can be converted by PK to pyruvate, which in turn serves as a substrate for PDH to produce acetyl-CoA for fatty acid synthesis.

ACKNOWLEDGMENTS

We thank D. Soldati (University of Geneva) and M. Meissner (University of Heidelberg) for the *T. gondii* TATi-line and Boris Striepen (University of Georgia) for pTetO7Sag4-ACP-cmyc-DHFR. We thank M. Parsons (University of Washington) and Boris Striepen (University of Georgia) for plasmids expressing mitochondrion- and apicoplast-targeted GFP/YFP fusion proteins. We are grateful to Stan Tomavo (University of Science and Technology, Lille) for providing anti-ENO1 and 2, Craig Roberts (Strathclyde University) for providing anti-ENR, and Keith Joiner (University of Arizona) for providing anti-NTPase.

This work was supported by a grant from the Deutsche Forschungsgemeinschaft (BO 1557/3-1).

REFERENCES

1. **Bendtsen, J. D., H. Nielsen, G. von Heijne, and S. Brunak.** 2004. Improved prediction of signal peptides: SignalP 3.0. J. Mol. Biol. **340:**783–795.
2. **Bisanz, C., O. Bastien, D. Grando, J. Jouhet, E. Marechal, and M. F. Cesbron-Delauw.** 2006. *Toxoplasma gondii* acyl-lipid metabolism: *de novo* synthesis from apicoplast-generated fatty acids versus scavenging of host cell precursors. Biochem. J. **394:**197–205.
3. **Black, M., F. Seeber, D. Soldati, K. Kim, and J. C. Boothroyd.** 1995. Restriction enzyme-mediated integration elevates transformation frequency and enables co-transfection of *Toxoplasma gondii*. Mol. Biochem. Parasitol. **74:**55–63.
4. **Crawford, M. J., N. Thomsen-Zieger, M. Ray, J. Schachtner, D. S. Roos, and F. Seeber.** 2006. *Toxoplasma gondii* scavenges host-derived lipoic acid despite its de novo synthesis in the apicoplast. EMBO J. **25:**3214–3222.
5. **DeRocher, A., C. B. Hagen, J. E. Froehlich, J. E. Feagin, and M. Parsons.** 2000. Analysis of targeting sequences demonstrates that trafficking to the *Toxoplasma gondii* plastid branches off the secretory system. J. Cell Sci. **113:**3969–3977.
6. **Donald, R. G., and D. S. Roos.** 1993. Stable molecular transformation of *Toxoplasma gondii*: a selectable dihydrofolate reductase-thymidylate synthase marker based on drug-resistance mutations in malaria. Proc. Natl. Acad. Sci. USA **90:**11703–11707.
7. **Dubey, J. P., D. S. Lindsay, and C. A. Speer.** 1998. Structures of *Toxoplasma gondii* tachyzoites, bradyzoites, and sporozoites and biology and development of tissue cysts. Clin. Microbiol. Rev. **11:**267–299.
8. **Dzierszinski, F., M. Mortuaire, N. Dendouga, O. Popescu, and S. Tomavo.** 2001. Differential expression of two plant-like enolases with distinct enzymatic and antigenic properties during stage conversion of the protozoan parasite *Toxoplasma gondii*. J. Mol. Biol. **309:**1017–1027.
9. **Eicks, M., V. Maurino, S. Knappe, U. I. Flügge, and K. Fischer.** 2002. The plastidic pentose phosphate translocator represents a link between the cytosolic and the plastidic pentose phosphate pathways in plants. Plant Physiol. **128:**512–522.
10. **Fast, N. M., J. C. Kissinger, D. S. Roos, and P. J. Keeling.** 2001. Nuclear-encoded, plastid-targeted genes suggest a single common origin for apicomplexan and dinoflagellate plastids. Mol. Biol. Evol. **18:**418–426.
11. **Fatland, B. L., B. J. Nikolau, and E. S. Wurtele.** 2005. Reverse genetic characterization of cytosolic acetyl-CoA generation by ATP:citrate lyase in Arabidopsis. Plant Cell **17:**182–203.
12. **Ferguson, D. J., D. Jacobs, E. Saman, J. F. Dubremetz, and S. E. Wright.** 1999. *In vivo* expression and distribution of dense granule protein 7 (GRA7) in the exoenteric (tachyzoite, bradyzoite) and enteric (coccidian) forms of *Toxoplasma gondii*. Parasitology **119:**259–265.
13. **Ferguson, D. J., S. F. Parmley, and S. Tomavo.** 2002. Evidence for nuclear localisation of two stage-specific isoenzymes of enolase in *Toxoplasma gondii* correlates with active parasite replication. Int. J. Parasitol. **32:**1399–1410.
14. **Ferguson, D. J., F. L. Henriquez, M. J. Kirisits, S. P. Muench, S. T. Prigge, D. W. Rice, C. W. Roberts, and R. L. McLeod.** 2005. Maternal inheritance and stage-specific variation of the apicoplast in *Toxoplasma gondii* during development in the intermediate and definitive host. Eukaryot. Cell **4:**814–826.
15. **Fichera, M. E., and D. S. Roos.** 1997. A plastid organelle as a drug target in apicomplexan parasites. Nature **390:**407–409.
16. **Fischer, K., B. Kammerer, M. Gutensohn, B. Arbinger, A. Weber, R. E. Häusler, and U. I. Flügge.** 1997. A new class of plastidic phosphate translocators: a putative link between primary and secondary metabolism by the phosphoenolpyruvate/phosphate antiporter. Plant Cell **9:**453–462.
17. **Fischer, K., and A. Weber.** 2002. Transport of carbon in non-green plastids. Trends Plant Sci. **7:**345–351.
18. **Flügge, U. I., R. E. Häusler, F. Ludewig, and K. Fischer.** 2003. Functional genomics of phosphate antiport systems. Physiol. Plant **118:**475–482.
19. **Foth, B. J., and G. I. McFadden.** 2003. The apicoplast: a plastid in *Plasmodium falciparum* and other apicomplexan parasites. Int. Rev. Cytol. **224:**57–110.
20. **Foth, B. J., L. M. Stimmler, E. Handman, B. S. Crabb, A. N. Hodder, and G. I. McFadden.** 2005. The malaria parasite *Plasmodium falciparum* has only one pyruvate dehydrogenase complex, which is located in the apicoplast. Mol. Microbiol. **55:**39–53.
21. **Funes, S., E. Davidson, A. Reyes-Prieto, S. Magallon, P. Herion, M. P. King, and D. Gonzalez-Halphen.** 2002. A green algal apicoplast ancestor. Science **298:**2155.
22. **Gornicki, P.** 2003. Apicoplast fatty acid biosynthesis as a target for medical intervention in apicomplexan parasites. Int. J. Parasitol. **33:**885–896.
23. **Gubbels, M. J., and B. Striepen.** 2004. Studying the cell biology of apicomplexan parasites using fluorescent proteins. Microsc. Microanal. **10:**568–579.
24. **Harb, O. S., B. Chatterjee, M. J. Fraunholz, M. J. Crawford, M. Nishi, and D. S. Roos.** 2004. Multiple functionally redundant signals mediate targeting to the apicoplast in the apicomplexan parasite *Toxoplasma gondii*. Eukaryot. Cell **3:**663–674.
25. **Harrison, D. J., and J. A. Langdale.** 2006. A step by step guide to phylogeny reconstruction. Plant J. **45:**561–572.
26. **Jelenska, J., M. J. Crawford, O. S. Harb, E. Zuther, R. Haselkorn, D. S. Roos, and P. Gornicki.** 2001. Subcellular localization of acetyl-CoA carboxylase in the apicomplexan parasite *Toxoplasma gondii*. Proc. Natl. Acad. Sci. USA **98:**2723–2728.
27. **Jomaa, H., J. Wiesner, S. Sanderbrand, B. Altincicek, C. Weidemeyer, M. Hintz, I. Turbachova, M. Eberl, J. Zeidler, H. K. Lichtenthaler, D. Soldati, and E. Beck.** 1999. Inhibitors of the nonmevalonate pathway of isoprenoid biosynthesis as antimalarial drugs. Science **285:**1573–1576.
28. **Kammerer, B., K. Fischer, B. Hilpert, S. Schubert, M. Gutensohn, A. Weber, and U. I. Flügge.** 1998. Molecular characterization of a carbon transporter in plastids from heterotrophic tissues: the glucose 6-phosphate/phosphate antiporter. Plant Cell **10:**105–117.
29. **Karnataki, A., A. Derocher, I. Coppens, C. Nash, J. E. Feagin, and M. Parsons.** 2007. Cell cycle-regulated vesicular trafficking of Toxoplasma APT1, a protein localized to multiple apicoplast membranes. Mol. Microbiol. **63:**1653–1668.
30. **Kissinger, J. C., B. Gajria, L. Li, I. T. Paulsen, and D. S. Roos.** 2003. ToxoDB: accessing the *Toxoplasma gondii* genome. Nucleic Acids Res. **31:** 234–236.
31. **Knappe, S., U. I. Flügge, and K. Fischer.** 2003. Analysis of the plastidic phosphate translocator gene family in Arabidopsis and identification of new phosphate translocator-homologous transporters, classified by their putative substrate-binding site. Plant Physiol. **131:**1178–1190.
32. **Kohler, S., C. F. Delwiche, P. W. Denny, L. G. Tilney, P. Webster, R. J. Wilson, J. D. Palmer, and D. S. Roos.** 1997. A plastid of probable green algal origin in apicomplexan parasites. Science **275:**1485–1489.
33. **Mazumdar, J., E. H. Wilson, K. Masek, C. A. Hunter, and B. Striepen.** 2006. Apicoplast fatty acid synthesis is essential for organelle biogenesis and parasite survival in *Toxoplasma gondii*. Proc. Natl. Acad. Sci. USA **103:**13192–13197.
34. **McMillan, P. J., L. M. Stimmler, B. J. Foth, G. I. McFadden, and S. Muller.** 2005. The human malaria parasite *Plasmodium falciparum* possesses two distinct dihydrolipoamide dehydrogenases. Mol. Microbiol. **55:**27–38.
35. **Meissner, M., D. Schluter, and D. D. Soldati.** 2002. Role of *Toxoplasma gondii* myosin A in powering parasite gliding and host cell invasion. Science **298:**837–840.
36. **Mullin, K. A., L. Lim, S. A. Ralph, T. P. Spurck, E. Handman, and G. I. McFadden.** 2006. Membrane transporters in the relict plastid of malaria parasites. Proc. Natl. Acad. Sci. USA **103:**9572–9577.
37. **Neuhaus, H. E., and M. J. Emes.** 2000. Nonphotosynthetic metabolism in plastids. Annu. Rev. Plant Physiol. Plant Mol. Biol. **51:**111–140.
38. **Ohlrogge, J., and J. Browse.** 1995. Lipid biosynthesis. Plant Cell **7:**957–970.
39. **Pandini, V., G. Caprini, N. Thomsen, A. Aliverti, F. Seeber, and G. Zanetti.** 2002. Ferredoxin-NADP$^+$ reductase and ferredoxin of the protozoan parasite *Toxoplasma gondii* interact productively in vitro and in vivo. J. Biol. Chem. **277:**48463–48471.
40. **Ralph, S. A., G. G. van Dooren, R. F. Waller, M. J. Crawford, M. J. Fraunholz, B. J. Foth, C. J. Tonkin, D. S. Roos, and G. I. McFadden.** 2004. Tropical infectious diseases: metabolic maps and functions of the *Plasmodium falciparum* apicoplast. Nat. Rev. Microbiol. **2:**203–216.
41. **Rangasamy, D., and C. Ratledge.** 2000. Compartmentation of ATP:citrate lyases in plants. Plant Physiol. **122:**1225–1230.
42. **Roos, D. S., R. G. Donald, N. S. Morrissette, and A. L. Moulton.** 1994. Molecular tools for genetic dissection of the protozoan parasite *Toxoplasma gondii*. Methods Cell Biol. **45:**27–63.
43. **Roos, D. S., M. J. Crawford, R. G. Donald, J. C. Kissinger, L. J. Klimczak, and B. Striepen.** 1999. Origin, targeting, and function of the apicomplexan plastid. Curr. Opin. Microbiol. **2:**426–432.
44. **Roughan, P. G., and J. B. Ohlrogge.** 1994. On the assay of acetyl-CoA synthetase activity in chloroplasts and leaf extracts. Anal. Biochem. **216:** 77–82.
45. **Silva-Filho, M. C.** 2003. One ticket for multiple destinations: dual targeting of proteins to distinct subcellular locations. Curr. Opin. Plant Biol. **6:**589–595.
46. **Soete, M., D. Camus, and J. F. Dubremetz.** 1994. Experimental induction of bradyzoite-specific antigen expression and cyst formation by the RH strain of *Toxoplasma gondii* in vitro. Exp. Parasitol. **78:**361–370.
47. **Thompson, J. D., T. J. Gibson, F. Plewiak, F. Jeanmougin, and D. G. Higgins.** 1997. The Clustal X windows interface: flexible strategies for multiple sequence alignment aided by quality analysis tools. Nucleic Acids Res. **25:**4876–4882.
48. **Tonkin, C. J., D. S. Roos, and G. I. McFadden.** 2006. N-terminal positively charged amino acids, but not their exact position, are important for apicoplast transit peptide fidelity in *Toxoplasma gondii*. Mol. Biochem. Parasitol. **150:**192–200.
49. **Waller, R. F., P. J. Keeling, R. G. Donald, B. Striepen, E. Handman, N. Lang-Unnasch, A. F. Cowman, G. S. Besra, D. S. Roos, and G. I. McFadden.** 1998. Nuclear-encoded proteins target to the plastid in *Toxoplasma gondii* and *Plasmodium falciparum*. Proc. Natl. Acad. Sci. USA **95:**12352–12357.
50. **Waller, R. F., S. A. Ralph, M. B. Reed, V. Su, J. D. Douglas, D. E.**

Minnikin, A. F. Cowman, G. S. Besra, and G. I. McFadden. 2003. A type II pathway for fatty acid biosynthesis presents drug targets in *Plasmodium falciparum*. Antimicrob. Agents Chemother. **47:**297–301.
51. **Waller, R. F., P. J. Keeling, G. G. van Dooren, and G. I. McFadden.** 2003. Comment on "A green algal apicoplast ancestor." Science **301:**49.
52. **Wiesner, J., and F. Seeber.** 2005. The plastid-derived organelle of protozoan human parasites as a target of established and emerging drugs. Expert Opin. Ther. Targets **9:**23–44.
53. **Yahiaoui, B., F. Dzierszinski, A. Bernigaud, C. Slomianny, D. Camus, and S. Tomavo.** 1999. Isolation and characterization of a subtractive library enriched for developmentally regulated transcripts expressed during encystation of *Toxoplasma gondii*. Mol. Biochem. Parasitol. **99:**223–235.